IEEE Access
Multidisciplinary | Rapid Review | Open Access Journal

Received September 29, 2017, accepted October 25, 2017, date of publication October 31, 2017,
date of current version November 28, 2017.

*Digital Object Identifier 10.1109/ACCESS.2017.2768389*

# Development of a Novel Hybrid-Type Rotary Steerable System for Directional Drilling

**JONGHEON KIM AND HYUN MYUNG, (Senior Member, IEEE)**
Urban Robotics Laboratory, Korea Advanced Institute of Science and Technology, Daejeon 34141, South Korea

Corresponding author: Hyun Myung (hmyung@kaist.ac.kr)

This work was supported in part by the Technology Innovation Program (Development of embedded directional drilling robot for drilling and exploration) through the Ministry of Trade, Industry & Energy, South Korea, under Grant 10076532 and in part by the Korean Ministry of Land, Infrastructure and Transport as the U-City Master and Doctor Course Grant Program.

**ABSTRACT** Unlike conventional resources, unconventional resources, such as shale gas and coal bed methane, are situated horizontally under geological formations. To exploit these resources, directional drilling and hydraulic fracturing technologies are required. In directional drilling, the dog leg severity (DLS), which indicates how much the angle changes while drilling 100 ft, is a major issue with respect to the cost and time of drilling. In this paper, we briefly review different types of directional drilling methods and propose a new hybrid-type rotary steerable system (RSS). DLS calculations based on three-point geometry for these systems are suggested. This hybrid RSS combining two conventional types of RSSs: point-the-bit and push-the-bit systems, achieves better steerability. The hybrid mechanism is implemented using hybrid pads with hydraulic cylinders and a spherical joint. The advantages of the proposed system are demonstrated by performing small-scale prototype and cement block drilling tests.

**INDEX TERMS** Directional drilling, dog leg severity (DLS), oil drilling, rotary steerable system (RSS), steering systems.

## NOMENCLATURE

| | |
|---|---|
| **CBM** | Coal Bed Methane |
| **RSS** | Rotary Steerable System |
| **DLS** | Dogleg Severity |
| **KOP** | Kick-off Point |
| **BHA** | Bottom-hole Assembly |
| **CAD** | Computer Aided Design |
| **WOB** | Weight on Bit |
| **RPM** | Revolutions per Minute |
| **ROP** | Rate of Penetration |
| **VD** | Vertical Depth |
| **HD** | Horizontal Departure |

## I. INTRODUCTION

The demand for extracting unconventional resources is rapidly increasing due to their large reserves. Shale gas reserves were estimated to be about 187.5 trillion $m^3$ in 2010, and potential reserves are expected to be about 635 trillion $m^3$ [1]. Unconventional resources such as shale gas are situated horizontally under geological formations; therefore, the most efficient way to excavate these resources is to use directional drilling and hydraulic fracturing technologies [2]. Directional drilling technology can reduce the drilling time and cost compared to those of conventional vertical drilling [3]. In oil and gas drilling, directional drilling also enables the avoidance of solid rocks located in underground paths and can be used for multi-target drilling and building multi-lateral wells from a single initial hole [4]. However, directional drilling is very challenging to perform succefully, because systems must withstand the high heat and pressure that exist deep underground [5], [6], which requires the use of technologies such as steering mechanisms, underground localization, and control algorithms. One of the key issues faced by directional drilling systems is dog leg severity (DLS). DLS expresses how much the drilling system angle (inclination and azimuth) changes while drilling a distance of 100 ft. As shown in Fig. 1, the kick-off point (KOP) becomes deeper as the DLS increases [7], which favorably affects the drilling time, cost, and productivity because vertical drilling using a top drive of the rig is faster than horizontal drilling using a mud motor in a bottom-hole assembly (BHA) and the exposed reservoir area is longer. Therefore, the deeper the KOP is, the shorter the directional drilling and the longer exposed reservoir distances are.

Directional drilling has been used in oil fields since the 1890s, from the inception of early whip-stock systems.

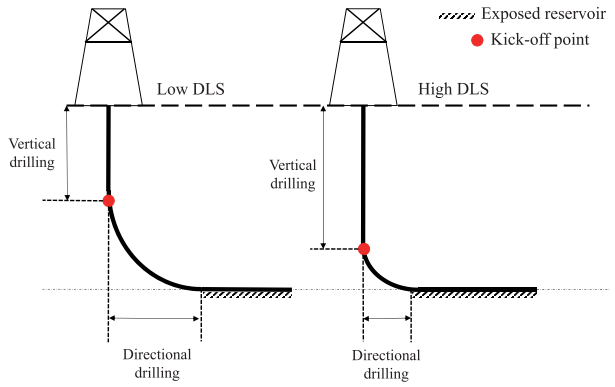


**FIGURE 1.** The effect of different DLS during directional drilling.

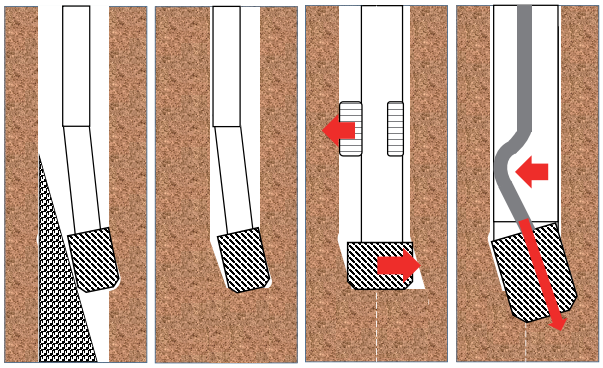

**FIGURE 2.** Types of directional drilling; from left, whip-stock, bent-sub, push-the-bit, and point-the-bit.

In the 1960s, a steerable motor (bent-sub) was developed. Directional drilling became more popular with the increase in demand to extract shale gas, and in the mid-1990s, RSSs began to appear [4], [10], [11]. Fig. 2 shows the schematic of these directional drilling methods. In the whip-stock method, an additional device composed of strong materials called a whip-stock is employed that has an incline and is used as a guide for the drilling direction. To apply a whip-stock to drilling, a large straight hole is drilled in advance, the drilling system is pulled out, the whip-stock is installed at the bottom of the borehole, and the drilling system is operated using a smaller drill bit. The drill bit follows the slope of the whip-stock and attains the desired steering angle for directional drilling. Although this method was the first directional drilling technique in the world, it has the drawback that the BHA needs to be pulled out from the hole whenever the drilling direction is changed, which increases the required drilling time and labor [10]. In the bent-sub system, the steering motor can deliver rotation power to the drill bit while bent. Consequently, the drilling time is shorter than that in the whip-stock method, since no additional equipment has to be installed; however, it is still necessary to pull the system out whenever a direction or angle change is necessary, because the bent angle cannot be adjusted while drilling [9], [11].

To address this problem, two types of rotary steerable systems, namely the push-the-bit and the point-the-bit systems, have been developed. Both types of systems can change direction while drilling, and as such, rotary steerable systems are the most convenient drilling systems available. In a push-the-bit system, three or four pads or blades that are equally spaced around the drill housing are employed to change the direction of the BHA. These pads both push the wellbore and move the center of the drill housing away from the wellbore. In a point-the-bit system, the drill bit heading is changed using a steering mechanism located inside the RSS. The proposed steering mechanism design is diverse and complicated in comparison with the push-the-bit type. The shape of the drill bit also differs from that of the push-the-bit system, in that a long gauge bit is used. Among directional drilling methods, the RSS is currently widely used due to its convenience and efficiency [18]–[21]. In 2013, Schlumberger Ltd. developed a hybrid RSS called the PowerDrive Archer [22]–[24]. It is a fully rotating RSS in which internal pads are used to move the drill housing by combining push-the-bit and point-the-bit systems. This system is expected to deliver a DLS of 18°/100ft, which indicates the best steerability among conventional RSSs.

In this paper, we propose a novel hybrid-type RSS. Our novel RSS concept is similar to the hybrid RSS developed by Schlumberger, but the proposed RSS is also able to pull the pad to the center of the drill housing, resulting in more net force for steering. The internal structures of the push-the-bit and point-the-bit systems are almost similar. Using this property, we propose a new type of RSS mechanism by combining mechanisms of these systems. This hybrid-type RSS can operate both steering mechanisms to provide more steering angle at the same time and needs only one actuator part for it. Then, we compare the maximum DLS of the proposed RSS to those of conventional RSSs by using three-point geometry. The maximum DLS for hole size of 171.5 mm and 216 mm achieved by major directional drilling companies is about 6.5°/100ft [8], [9]. Two novel RSS prototypes are developed during our study; one for a laboratory-scale experiment using electronic motors and another for a cement block drilling experiment using a real-scale model using hydraulic cylinders. Two experiments are performed to demonstrate the steerability of the developed systems, and a simple schematic of the developed directional drilling system components is provided in Fig. 3. The BHA is composed of five parts: a drill pipe, a sensing and control unit, a mud motor, a steering unit, and a drill bit. The contribution of this paper is the proposal and development of a novel hybrid-type rotary steerable system (RSS) which can achieve high DLS compared to the conventional drilling system.

## II. HYBRID TYPE RSS

In oil fields, the drilling length is extended by connecting drilling pipes; as the length and depth of drilling increase, more pipes and force are required [12]. The sensing/control unit is designed to estimate the location of the system and

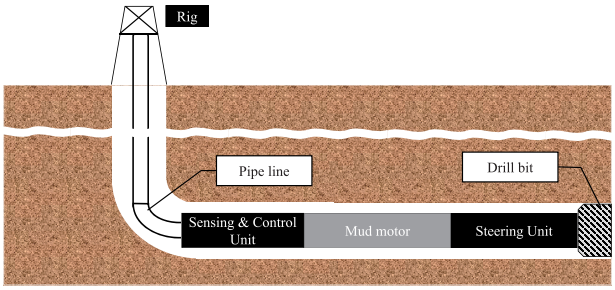


**FIGURE 3.** Schematic of directional drilling system.

to control its direction [13]. A mud motor located between the sensing/control unit and steering unit, produces rotation power by converting mud pressure into torque. The steering unit is equipped with hybrid pads that push the wellbore and tilt the drill bit. Finally, the drill bit is used to crush or cut rocks. While correct bit selection is an important factor in drilling because it affects the rate of penetration (ROP) [14], only the steering unit is discussed in this paper. We focus on the design of the steering unit mechanism and its control, which is the first option for improving the DLS of the RSS when using geometric methods [15]–[17].

One of the main issues in directional drilling is the DLS. Drilling vertically with a top drive rig is faster than using a mud motor underground, and thus a high DLS can decrease the horizontal departure and overall drilling time. Our proposed hybrid type RSS is a combination of push-the-bit and point-the-bit systems, thus providing high steerability through utilization of hybrid pads. This system is equipped with three hybrid pads that can tilt the drill string inside the housing and push the outer wall, which is possible due to the operating structure of combining two types of RSSs. For both types, when the RSS is being steered while going forward, a force must be applied to the side opposite to the system heading. Taking this factor into consideration, we designed new pads that can actuate both push-the-bit and point-the-bit systems simultaneously, as shown in Fig. 4(a).

As can be seen in Fig. 4(c), each pad operates with a cylinder that moves parallel to the drill shaft. The pad only moves perpendicularly, as it is connected to a guide rail that is fixed to the drill housing. The pad has a slope inside its body, and bearings are attached at the end of the cylinder rod to transform parallel movement into perpendicular movement. These pads push the wellbore and drill shaft simultaneously to move of the proposed RSS.

There are some design considerations for the proposed RSS. In each drilling technique, mud is used to cool the drill bit, to remove fragments that spring up during drilling, and to drive the mud motor. Therefore, a drilling system should have a mud path to allow mud to pass through. As shown in Figs. 4(b) and 4(d), mud enters the steering unit immediately after passing through the mud motor. First, mud flows into the chamber, which builds the mud pressure to activate the cylinder via the pressure valve. The pressure valve consists of a screw, tab, and spring, and controls the internal pressure of the steering unit by blocking mud flow until the pressure reaches a set value. Given the inner diameter of the chamber $D_c$, spring constant $k_s$, distance between the block and the chamber's exit $\Delta d$, and initial tension of the spring $T_i$, the generated pressure $P_c$ can be represented as:

$$P_c = \frac{F_s}{A} = \frac{4 \cdot (k_s \cdot \Delta d + T_i)}{\pi \cdot {D_c}^2} \tag{1}$$

where $A$ is the cross-sectional area of the inner chamber and $F_s$ is the force from the spring. The distance $\Delta d$ can be changed by adjusting the pressure valve. The drill shaft is separated into three links with two universal joints, and the drill shaft can thus be bent into any desired position without being damaged. However, the mud cannot flow through the universal joint; thus, mud inside the chamber flows to the inside of the steering unit housing until it reaches the bit box. When the mud reaches the bit box, it flows into the bit box and sprays out from the bit. Since there are numerous bearings inside the steering unit, rubber seals are employed to prevent bearing abrasion.

## III. CONTROL AND DLS

### A. DIRECTIONAL CONTROL OF THE HYBRID RSS

The drill shaft is controlled by three different pads pointing toward the center of the drill housing. Each pad is controlled by a hydraulic system, which consists of a four-port–three-way solenoid valve and a hydraulic cylinder. As illustrated in Fig. 5(a), given the desired position to the center of the drill shaft, we use a rotation matrix to control the position of each pad. The coordinate of the target point is $(x, y)$ and the angles between the $X$–axis and pad axes $l_1$, $l_2$, and $l_3$ are $\alpha$, $\beta$, and $\gamma$, respectively. Assuming that the vector $A$ contains the coordinates in a relative coordinate frame located on axis $l_1$, the vector $B$ contains the coordinates in a global coordinate frame, and the matrix $R$ is the rotation matrix around $Z$–axis, the relationship between $A$ and $B$ can be written as:

$$A = R^{-1}B = \begin{bmatrix} \cos\alpha & -\sin\alpha & 0 \\ \sin\alpha & \cos\alpha & 0 \\ 0 & 0 & 1 \end{bmatrix}^{-1} \begin{bmatrix} x \\ y \\ 0 \end{bmatrix} \tag{2}$$

where $A = [x_1\ y_1\ 0]^T$, $B = [x\ y\ 0]^T$.

**TABLE 1.** Relationship between global and relative coordinates.

| Target point | On axis $l_1$ | On axis $l_2$ | On axis $l_3$ |
|---|---|---|---|
| $x$ | $-x\cos\alpha$ | $-x\cos\beta$ | $-x\cos\gamma$ |
| $y$ | $-y\sin\alpha$ | $-y\sin\beta$ | $-y\sin\gamma$ |

Table 1 shows the relationship between the global coordinate frame and the relative coordinates on each axis $l_1$, $l_2$, and $l_3$ when $(x,y)$ is on the global coordinate frame. By applying the same equations to pads 2 and 3, the distances $d_1$, $d_2$, and $d_3$ that the three pads must move can be obtained as follows:

$$d_1(t+1) = d_1(t) - (x\cos\alpha + y\sin\alpha) \tag{3}$$
$$d_2(t+1) = d_2(t) - (x\cos\beta + y\sin\beta) \tag{4}$$
$$d_3(t+1) = d_3(t) - (x\cos\gamma + y\sin\gamma) \tag{5}$$

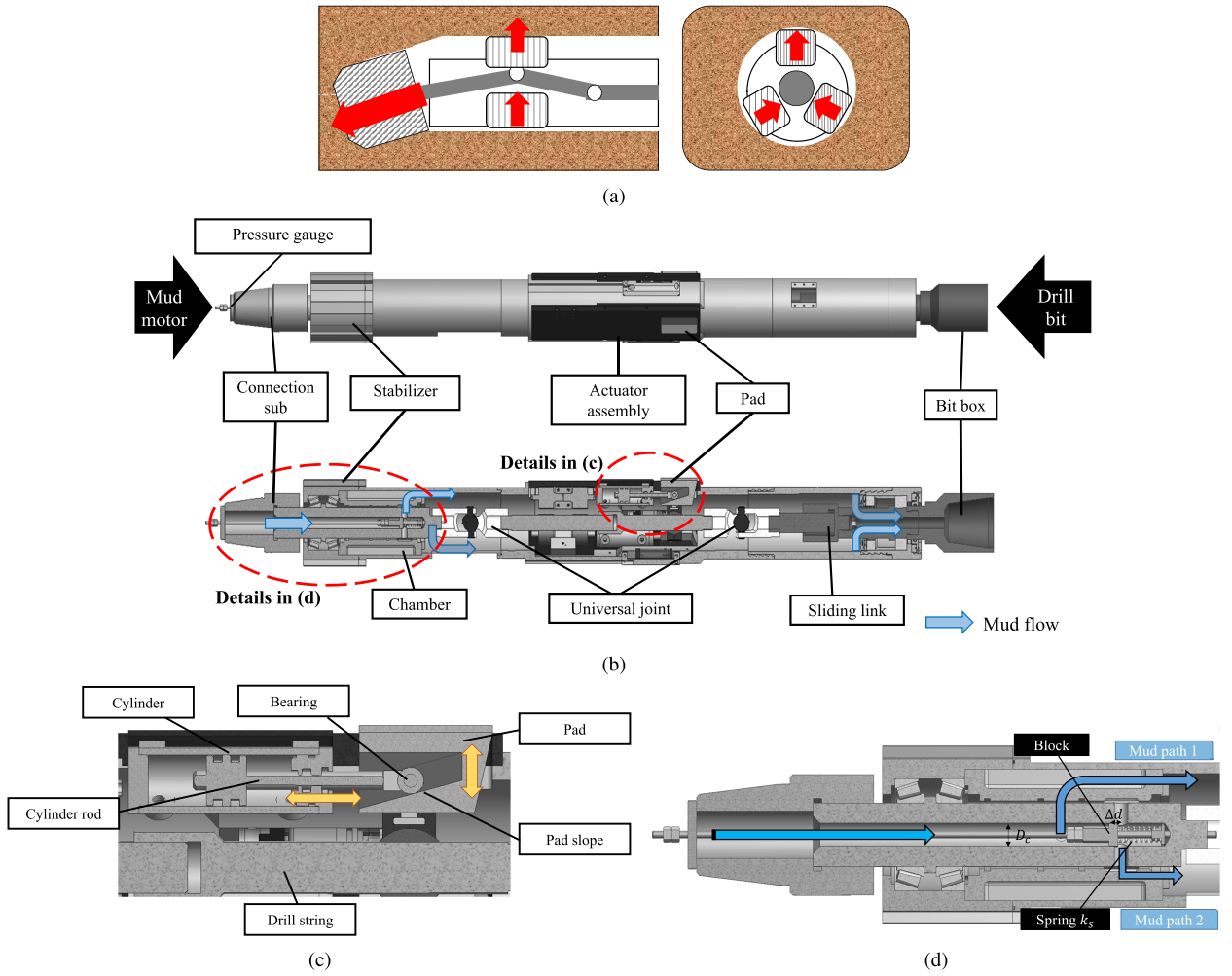


**FIGURE 4.** (a) Concept design of the proposed RSS. (b) CAD model of the steering unit of the proposed RSS. (c) Structures of a hybrid pad and cylinder for the proposed RSS. (d) Structure of the pressure generator and mud flow (Mud path 1: mud flow into the actuator assembly, Mud path 2: mud flow into the inner drill housing after mud pressure is generated).

where $d_1(t)$, $d_2(t)$, and $d_3(t)$ are the current positions of the pads, and $d_1(t+1)$, $d_2(t+1)$, and $d_3(t+1)$ are the new positions of the pads when the center of the drill shaft moves to $(x, y)$. An encoder is installed between each pad and the drill housing, and its value is used for feedback control. After the positions of the pads are determined, all three pads should move simultaneously without damaging the cylinders. We therefore divided the movement into $n$-steps. For example, if the center of the shaft is located at the center of the housing and is about to move to $(x, y)$, a direct straight-line path is drawn and its length is divided into $n$-steps. Hence, the three pads undergo only small movements in each step to decrease the mechanical load on the cylinders. The pad positions are confirmed and compensated based on the encoder values in each step.

### B. DLS CALCULATIONS

As previously mentioned, the DLS represents the performance of an RSS as an angle per 100 ft or 30 m. The units of length and angle are meters and radians in equations (6) to (18) unless otherwise stated. There are several theoretical methods for calculating DLSs. The first method is to use the vertical depth (VD) and horizontal departure (HD) [4]. As can be seen in Fig. 6, it is assumed in this method that the radius of the curvature $R$ remains unchanged.

$$DLS = \frac{360 \times 30}{2\pi R} \tag{6}$$

$$VD = R \sin\theta \tag{7}$$

$$HD = R(1 - \cos\theta) \tag{8}$$

where $\theta$ is the curvature angle of the drill trajectory. However, this method is usually employed for setting the drilling path and can be utilized to calculate the DLS only after drilling.

The second method for calculating the DLS is called the three-point geometry method, and it can be applied to bent-sub and point-the-bit drilling systems as they operate using similar mechanisms. The three points of contact that establish a curve are the drill bit, kick pad, and top stabilizer for

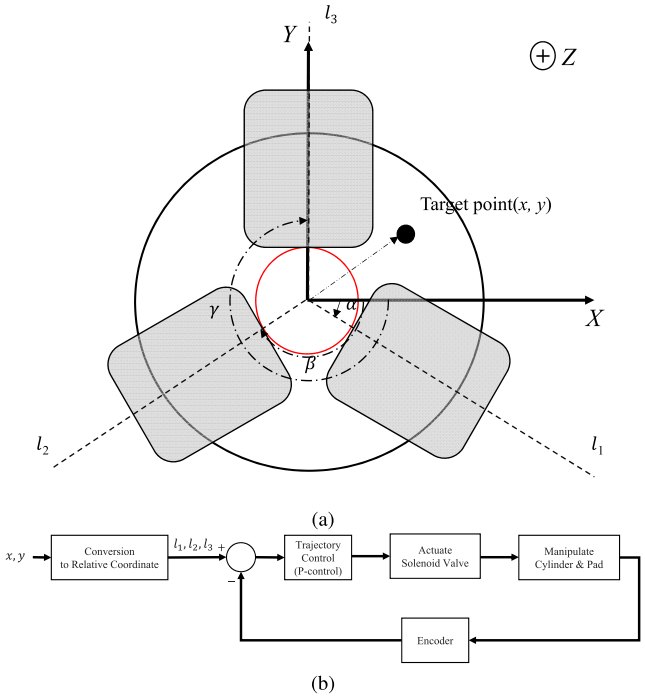


**FIGURE 5.** (a) Schematic of the pads and drill shaft. (b) RSS control diagram.

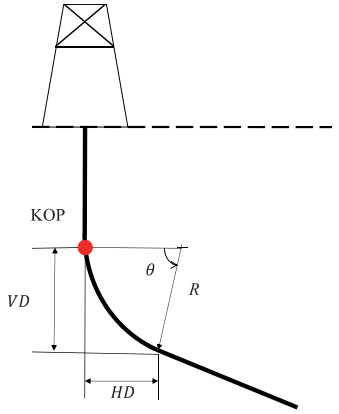


**FIGURE 6.** Simple diagram for DLS calculation.

a bent-sub system. Calculation of the DLS of the system is dependent on the following components: the bent angle, outer diameter of the stabilizer, location of the top stabilizer in the BHA, and distance between the bit gauge and bent point. Fig. 7(a) presents a diagram of the three-point geometry method for a bent-sub system [25]. For a point-the-bit system, it can be assumed that the near bit stabilizer is a bent point. These three points form a triangle and by using the law of sines, the radius of curvature $R$ and the DLS can be calculated as follows:

$$R = \frac{L}{2\sin(\pi-\theta)} \approx \frac{L_1+L_2}{2\sin\theta} \tag{9}$$

$$DLS = \frac{180}{\pi}\cdot\frac{100}{R} \approx \frac{36000\theta}{\pi(L_1+L_2)}. \tag{10}$$

To obtain the DLS of the push-the-bit type, three-point contact geometry can also be applied. As shown in Fig. 7(b), three contact points are between a wellbore and a top stabilizer ($P_1$), the BHA housing ($P_2$), and the drill bit ($P_3$). Let us denote the diameters of the drill bit, the BHA housing, and the stabilizer as $D_b$, $D_h$, and $D_s$, respectively, and the distance between the drill bit and the stabilizer as $D$. These three points are the vertices of a triangle whose circumcircle has the radius of the borehole curvature $R$, which can be determined using a Pythagorean theorem and the DLS can be approximated as follows:

$$R \approx \frac{B^2+(\frac{B\cdot D}{A+B})^2}{2B} \tag{11}$$

$$DLS \approx \frac{360}{\pi}\cdot\frac{30\cdot B}{B^2+(\frac{B\cdot D}{A+B})^2} \tag{12}$$

where $A = \frac{D_s-D_h}{2}$, $B = \frac{D_b-D_h}{2}$, and $C = \frac{BD}{A+B}$.

However, this method is not suitable for showing the effect of the pad position. According to a study by Zhang and Samuel [16], an analytical model for the push-the-bit system can be obtained, as shown in Fig. 7(c). This model also has three contact points, which are located at; the stabilizer ($P_1$), the pad ($P_2$), and the bit ($P_3$). In Fig. 7(c), $\alpha_1$ is the angle between the two lines: one is formed by connecting contact points $P_2$ and $P_3$, the other is the horizontal line passing through $P_2$. Similarly, $\alpha_2$ is the angle between the two lines: one is formed by connecting contact points $P_1$ and $P_2$, the other is the horizontal line passing through $P_2$. The distances between axis of the BHA and the contact points are denoted as $d_1$, $d_2$, and $d_3$. $L_1$ and $L_2$ represent the distances between the bit and the pad; and between the pad and the stabilizer, respectively. Next, the DLS of a push-the-bit system can be calculated from the ratio between the angular change $\alpha$ and travelled length $L$, which is then converted into degrees per 30 m as follows:

$$\alpha = \alpha_1+\alpha_2 \approx \frac{d_2-d_3}{L_1}+\frac{d_1-d_3}{L_2} \tag{13}$$

$$DLS \approx \frac{\alpha}{L}\cdot\frac{30\cdot\pi}{180} = \frac{\frac{d_2-d_3}{L-1}+\frac{d_1-d_3}{L_2}}{L_1+L_2}\cdot\frac{30\cdot\pi}{180}. \tag{14}$$

The designed novel RSS can be regarded as a push-the-bit system with an additional bent angle $\alpha$. Three contact points exist between the wellbore and RSS, which are located at: the stabilizer, the pad, and the drill bit. A simple diagram depicting this RSS is presented in Fig. 7(d). To obtain the DLS of the newly designed RSS, it is necessary to calculate $R$. The dimensions $A$, $B$, and $D_1$ can be expressed in terms of the radius of the pad $R_P$ when it reaches the point of maximum stroke, the radius of the drill bit $R_D$, the radius of the stabilizer $R_S$, the distance between the pad and the drill bit $L_1$, the distance between the pad and the stabilizer $D_2$, and the bent angle $\alpha$ as follows:

$$A = R_P - R_S \tag{15}$$

$$B = R_P + L_1\sin\alpha - R_D\cos\alpha \tag{16}$$

$$D_1 = L_1\cos\alpha + R_S\sin\alpha. \tag{17}$$

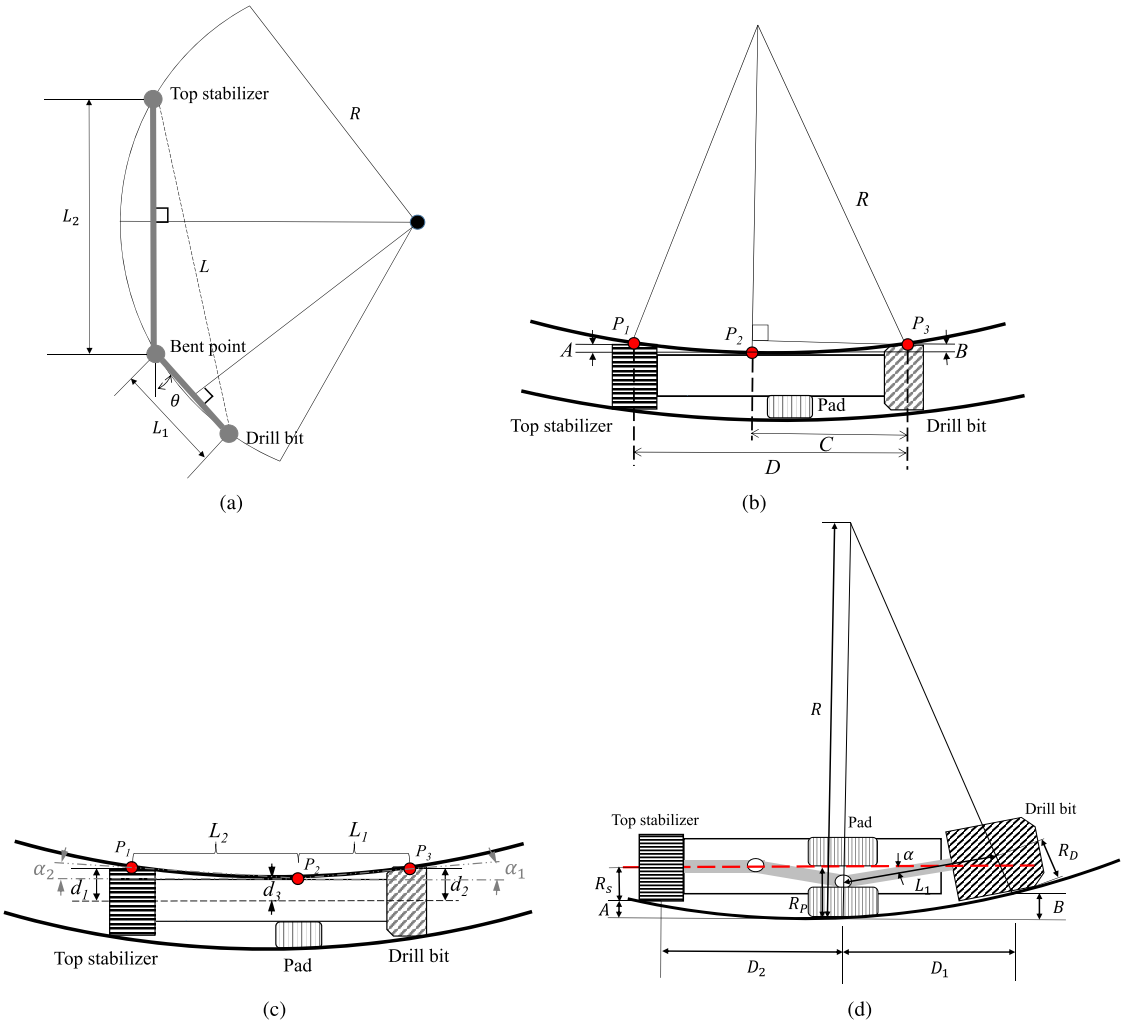


**FIGURE 7.** Diagrams of the three-point geometry for (a) a bent-sub system. (b) a push-the-bit system. (c) a push-the-bit system including the pad position. (d) a hybrid system.

Applying these parameters to (12), the DLS of the hybrid RSS can be obtained as follows:

$$DLS \approx \frac{360}{\pi} \cdot \frac{30 \cdot B}{B^2 + \{\frac{B(D_1+D_2)}{A+B}\}^2}. \tag{18}$$

Equation (18) can also be applied to point-the-bit RSSs (assuming that $R_P$ is the same as the radius of the drill housing) and push-the-bit RSSs (if $\alpha = 0$).

### C. DLS COMPARISON

It is necessary to compare the DLS of the push-the-bit, the point-the-bit, and hybrid RSSs to prove the advantages of the proposed hybrid RSS. Fig. 8(a) shows how the DLS changes with the position of the steering mechanism in systems of the three RSS types when the total system length is 3 m. The installation location of the steering unit ($L_1$) is from 2 ft to 8 ft due to the size of the drill bit and the stabilizer. The steering angle, cylinder stroke, radius of housing, radius of stabilizer, and radius of drill bit are 1.7°, 10.4 mm, 85.7 mm, 102.5 mm, and 111 mm, respectively. In this case, the steering angle should be 0° for the push-the-bit system and the cylinder stroke should be regarded as 0 mm for the point-the-bit system. For the point-the-bit system and the hybrid RSS, the DLS value is proportional to the distance between the bit and steering mechanism; however, a longer gauge bit is required to achieve a greater DLS. The DLS of the push-the-bit system is favorable when the steering mechanism is close to the bit; otherwise, it is lower than the DLSs of the other types of systems. As expected, the hybrid RSS yielded a DLS better than those of the other systems. Fig. 8(b) shows the steering efficiency of the hybrid RSS over the maximum DLS of the other RSSs.

## IV. DRILLING EXPERIMENTS

### A. LABORATORY-SCALE DRILLING EXPERIMENT (PROTOTYPE RSS)

We built a prototype to test the DLS capability of the proposed RSS on the laboratory-scale. A drilling experiment was conducted using high-density insulation foam with a length,

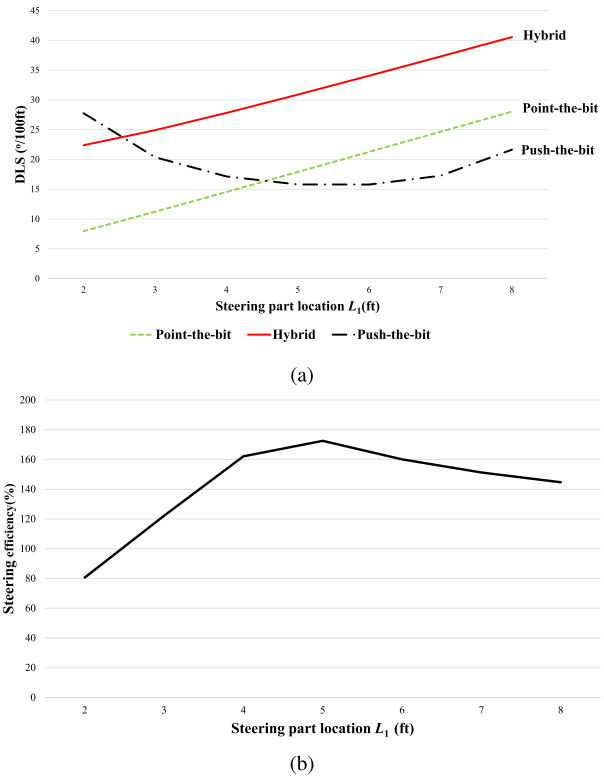


**FIGURE 8.** (a) Comparison of DLSs obtained using different steering part location ($L_1$). (b) Steering efficiency of the hybrid RSS over the maximum DLS of the other RSSs.

width, and height of 7.2 m, 1 m, and 0.9 m, respectively. The compressive strength of the insulation foam was approximately 0.5 MPa. Fig. 9(a) shows the settings employed in the prototype drilling experiment. We used a scissor jack to supply weight on bit (WOB) to the system and made gantries to hold the drilling point. The mechanism of the prototype RSS was similar to that of a real-scale RSS, but was scaled down to 1/3 size, and electric power was used to move the pads and drill bit. To estimate its DLS, it was necessary to determine several specifications for the prototype RSS. Table 2 and Fig. 9(b) provide the specifications and an image of the designed prototype RSS. By substituting these parameters into (11)–(18), the DLS was predicted to be approximately 67.9°/100ft.

The experimental procedure was as follows:

1) Align the gantry with the desired drilling direction.
2) Place the RSS on the gantry.
3) Drill with the RSS until the middle of the pad reaches the surface of the insulation foams.
4) Move the pad out to the maximum point in the desired direction.
5) Continue drilling and attaching pipe lines until the bit reaches the end of the insulation foams.
6) Pull out the RSS and check the hole position between foam blocks by breaking them apart.

Figs. 9(c) and (d) present the results of the drilling experiment in which each foam block was 1.8 m long.

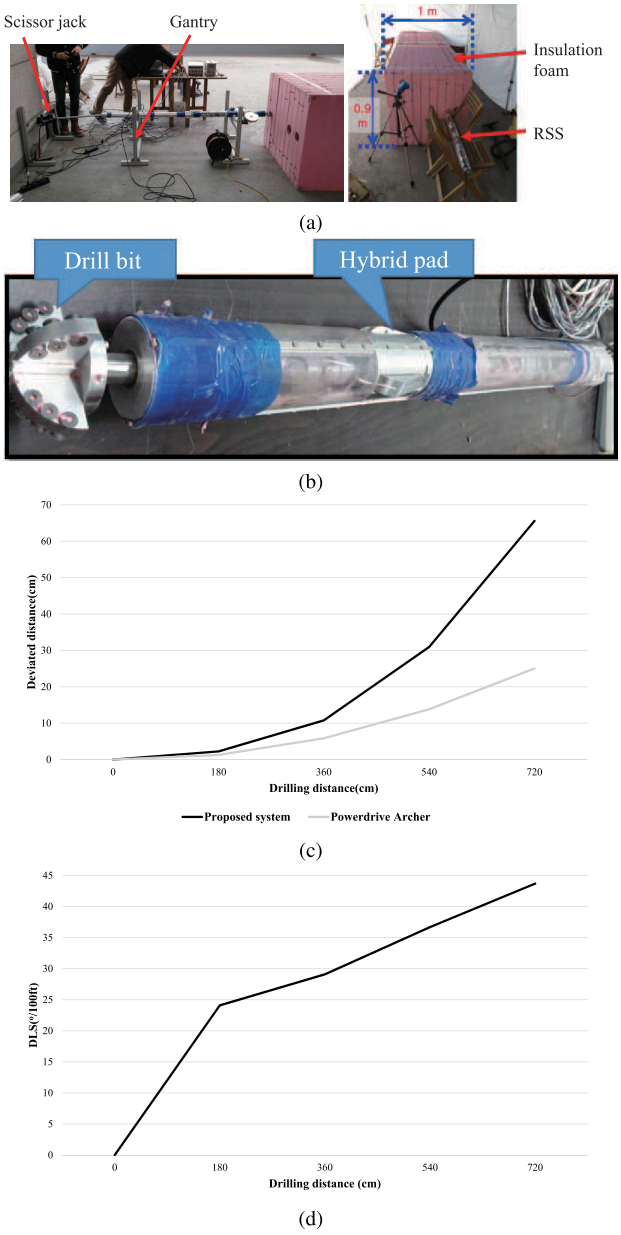


**FIGURE 9.** (a) Experimental settings used in the laboratory-scale test. (b) 1/3-scale prototype of the proposed RSS. (c) Deviated distance in the small-scale drilling test compared with the highest DLS achieved from a conventional RSS. (d) DLS of the small-scale drilling test.

The prototype RSS achieved a maximum DLS of approximately 43.7°/100ft. We set the drilling direction to the left of the RSS, but the results indicate that the RSS drilled out to the bottom left. This difference was resulted from the fact that when the friction force between the insulation foam and drill bit exceeds that between the insulation foam and other parts of the RSS, the torque from the motor inside the RSS rotates the body of the RSS.

### *B. CEMENT BLOCK DRILLING EXPERIMENT (REAL-SCALE RSS)*

The developed RSS was designed to drill cube-shaped cement blocks each having dimensions of 1 m × 1 m × 1 m.

**TABLE 2. Specification of the small-scale RSS.**

| | |
|---|---|
| Total length ($L$) | 953 mm |
| Max. pad stroke ($s$) | $\pm$10 mm |
| Max. bent angle ($\alpha$) | 3.55° |
| Radius of housing ($R_H$) | 35 mm |
| Radius of pad with max. stroke ($R_P = R_H + s$) | 45 mm |
| Radius of drill bit ($R_D$) | 42 mm |
| Radius of stabilizer ($R_S$) | 35 mm |
| Distance between bit and pad ($L_1$) | 237 mm |
| Distance between pad and stabilizer ($L_2$) | 716 mm |

Ten cement blocks were used with two different compressive strengths: five each with compressive strength of 40 MPa and 55 MPa. Fig. 10(a) shows the testbed settings. Additional equipment utilized during the experiment included a horizontal drill rig, a mud pump, and a mud motor. We changed a general vertical rig into a horizontal drill rig that could apply a maximum pressure of 20 MPa to the BHA and included a rotary table to attach or detach pipes. The mud pump provides mud to the mud motor with a hydraulic pressure of up to 2 MPa and a flow rate of 1,500 *l*/min. We used a conventional mud motor with the same outer diameter as the steering unit housing (172 mm), a rotary speed of 112–163 rpm, a working pressure loss of 4.2 MPa, and a required flow rate of 1,324–1,930 *l*/min. As can be seen from the specifications of the mud pump and the mud motor, those of the mud motor exceed those of the mud pump. No mud pump with better specification was available, and the performance of the mud motor was been degraded. For example, the rotary speed of the mud motor dropped to 67 rpm after connecting and testing with the mud pump. Additionally, the hydraulic cylinders could not supply enough side force to the drill bit due to insufficient supply of mud pressure in the chamber. The mud pressure dropped to almost zero after it passed through the mud motor. Table 3 summarizes the main specification for the designed RSS and Fig. 10(b) shows an image of the designed steering unit of the RSS. By applying (11)–(18), the DLS can be predicted to be approximately 38.96°/100ft, which is roughly double that of conventional RSSs in terms of steerability.

The experimental procedure was as follows:

1) Set the alignment of the drilling system components: the rig, support fixture, and RSS.
2) Drill with the RSS until the middle of the pad reaches the surface of the cement block.
3) Move the pad out to the desired direction with maximum stroke.
4) Continue drilling and attaching pipe lines until the bit reaches the end of the cement blocks.
5) Pull out the RSS and check the hole position between cement blocks by disassembling the concatenated blocks.

Figs. 10(c) and (d) show the results obtained from drilling the cement blocks. The installed cement blocks were 10 m long in total and the kick-off started around 1 m. However, after drilling 9 m, the drill bit hit the top of the fixed base.

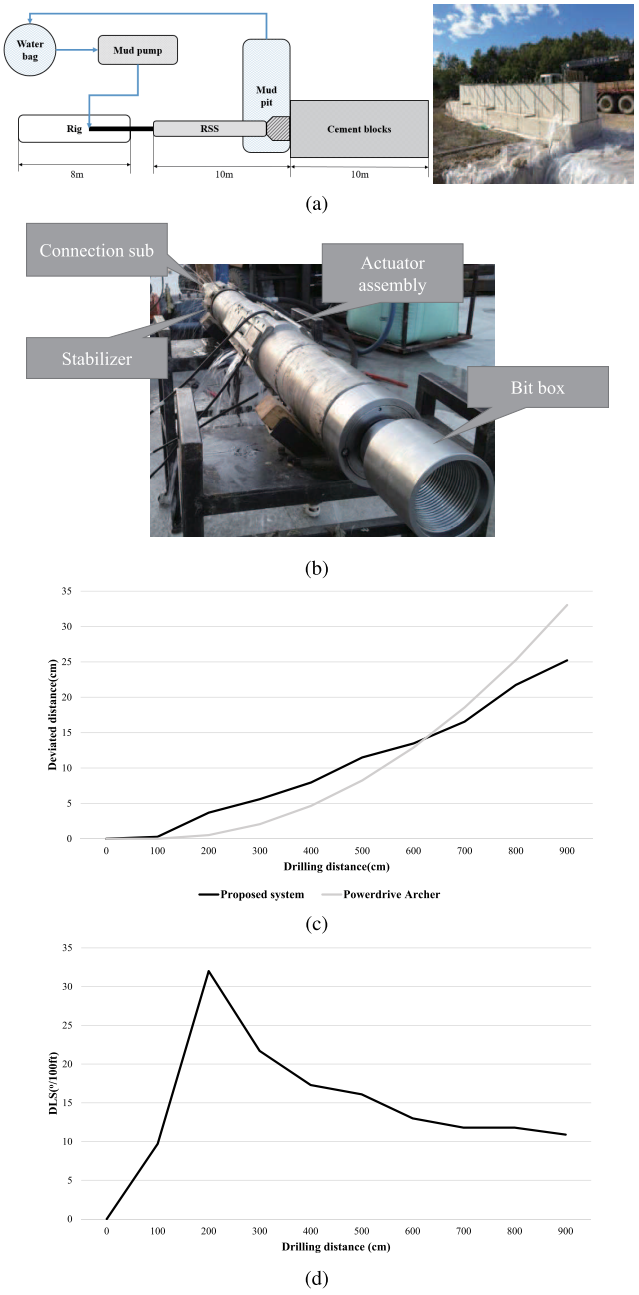


**FIGURE 10. (a) Testbed and settings for the cement block drilling test. (b) Picture of the developed steering unit. (c) Deviated distance in the cement block drilling test compared with the highest DLS achieved from a conventional RSS. (d) DLS changes from the cement block drilling test.**

The RSS achieved a maximum DLS of about 32.0°/100ft when drilling the second block. We set the drilling direction to the right side of the RSS, but the results show that the RSS drilled out to the bottom right due to gravity and the friction between the drill bit and cement blocks similar to the laboratory-scale experiment results. In addition, the DLS decreases significantly with deeper drilling, due to a change of the compressive strength of the cement blocks and sludge inside the borehole because of insufficient mud flow from the mud motor. This problem can be improved by switching

**TABLE 3. Specification of the real-scale RSS.**

| | |
|---|---|
| Total length ($L$) | 1,875 mm |
| Max. pad stroke ($s$) | $\pm$10.5 mm |
| Max. bent angle ($\alpha$) | 1.7° |
| Radius of housing ($R_H$) | 86 mm |
| Radius of pad with max. stroke ($R_P = R_H + s$) | 90.5 mm |
| Radius of drill bit ($R_D$) | 111.13 mm |
| Radius of stabilizer ($R_S$) | 102.5 mm |
| Distance between bit and pad ($L_1$) | 1,000 mm |
| Distance between pad and stabilizer ($L_2$) | 1,475 mm |

to a mud pump with superior specification. However, the experimental results reflect good DLS performance despite this problem.

## V. CONCLUSION

We proposed and developed a novel hybrid RSS mechanism with high steerability (up to 32°/100ft). The DLS values of three types of RSSs were compared to that of the hybrid RSS. The developed system produced the best results in terms of steerability and was less affected by formation hardness due to simultaneous operation of point-the-bit and push-the-bit mechanisms. We also proposed a method of calculating the DLS of the hybrid RSS using three-point geometry. To determine the DLS accurately, additional factors such as the number of revolutions per minute (RPM), side force of the drill bit and ROP of the BHA should be considered [17], [26]. According to experiments conducted by Sugiura [15], the ideal drill bit RPM is 100 and the ideal BHA ROP is approximately 15 m/hr. Unfortunately, our prototype RSS was operated at 67 rpm and 1.28 m/hr during the experiment. The results of the experiment will approach the theoretical values if the drill bit RPM and BHA ROP are increased. In future works, the proposed RSS mechanism should be optimized in terms of system composition and directional stability. We will also develop an angle holding algorithm using the roll angle of the BHA housing to hold its drilling direction and to follow planned path. In addition, we would like to improve the bit design, pressure control, and rotating torque to achieve better system performance.

## REFERENCES

[1] V. Kuuskraa, S. Stevens, T. van Leeuwen, and K. Moodhe, *World Shale Gas Resources: An Initial Assessment of 14 Regions Outside the United States*. Washington, DC, USA: United States Energy Information Administration, 2011.

[2] C. Zheng *et al.*, "Research on the effect of gas nitriding treatment on the wear resistance of ball seat used in multistage fracturing," *Mater. Des.*, vol. 70, pp. 45–52, Apr. 2015.

[3] T. Inglis, *Directional Drilling*. Berlin, Germany: Springer, 2013.

[4] J. Choi, *Offshore Drilling Engineering*. Seoul, South Korea: CIR, 2012.

[5] X. Li, S. Wang, R. Malekian, S. Hao, and Z. Li, "Numerical simulation of rock breakage modes under confining pressures in deep mining: An experimental investigation," *IEEE Access*, vol. 4, pp. 5710–5720, Sep. 2016.

[6] C. Zhang, W. Zou, and N. Cheng, "Overview of rotary steerable system and its control methods," in *Proc. IEEE Int. Conf. Mechatronics Autom.*, Harbin, China, Aug. 2016, pp. 1559–1565.

[7] B. Park, J. Kim, J. Park, J.-U. Shin, and H. Myung, "Hybrid 4-pad rotary steerable system for directional drilling of unconventional resources," in *Proc. Ubiquitous Robots Ambient Intell. (URAI)*, Jeju, South Korea, Oct./Nov. 2013, pp. 659–660.

[8] H. M. Khattab *et al.*, "High build up rate rotary steerable system leads to revolutionize onshore horizontal drilling in western desert of egypt," in *Proc. SPE/IADC Middle East Drilling Technol. Conf. Exhib.*, Abu Dhabi, UAE, Jan. 2016, pp. 1–8.

[9] A. A. Dabyah, E. Biscaro, and H. Mayer, "New generation of rotary steerable system enables higher BUR and performance," in *Proc. SPE Annu. Tech. Conf. Exhib.*, Dubai, UAE, Sep. 2016, pp. 1–10.

[10] E. Noveiri and A. T. Nia, "Directional drilling optimization by non-rotating stabilizer," *Int. J. Mech. Aerosp. Ind. Mech. Manuf. Eng.*, vol. 5, no. 1, pp. 329–336, Mar. 2011.

[11] G. Downton, T. Klausen, A. Handriks, and D. Pafitis, "New directions in rotary steerable drilling," *Oilfield Rev.*, vol. 12, no. 1, pp. 18–29, Mar. 2000.

[12] H. Omori, T. Murakami, H. Nagai, T. Nakamura, and T. Kubota, "Development of a novel bio-inspired planetary subsurface explorer: Initial experimental study by prototype excavator with propulsion and excavation units," *IEEE/ASME Trans. Mechatronics*, vol. 18, no. 2, pp. 459–470, Apr. 2013.

[13] B. Park and H. Myung, "Underground localization using dual magnetic field sequence measurement and pose graph SLAM for directional drilling," *Meas. Sci. Technol.*, vol. 25, no. 12, p. 125101, Oct. 2014.

[14] H. Rabia, M. Farrlly, and M. Barr, "A new approach to drill bit selection," in *Proc. SPE Eur. Petroleum Conf.*, London, U.K., Oct. 1986, pp. 1–8.

[15] J. Sugiura, "Optimal BHA design for steerability and stability with configurable rotary-steerable system," in *Proc. SPE Asia Pacific Oil Gas Conf. Exhib.*, Perth, Australia, Oct. 2008, pp. 1–13.

[16] Y. Zhang and R. Samuel, "Analytical model to estimate the directional tendency of point and push-the-bit BHAs," in *Proc. SPE Annu. Tech. Conf. Exhib.*, Houston, TX, USA, Sep. 2015, pp. 1–12.

[17] S. F. Noynaert and E. Gildin, "Going beyond the tally book: A novel method for analysis, prediction and control of directionally drilled wellbores using mechanical specific energy," in *Proc. SPE Annu. Tech. Conf. Exhib.*, Amsterdam, The Netherlands, Oct. 2014, pp. 1–18.

[18] T. Yonezawa *et al.*, "Robotic controlled drilling: A new rotary steerable drilling system for the oil and gas industry," in *Proc. IADC/SPE Drilling Conf.*, Dallas, TX, USA, Feb. 2002, pp. 1–15.

[19] S. Menand *et al.*, "PDC bit steerability modeling and testing for push-the-bit and point-the-bit RSS," in *Proc. IADC/SPE Drilling Conf. Exhib.*, San Diego, CA, USA, Mar. 2012, pp. 1–12.

[20] S. Poli, F. Donati, J. Oppelt, and D. Ragnitz, "Advanced tools for advanced wells: Rotary closed loop drilling system—Results of prototype field testing," *SPE Drilling Completion*, vol. 13, no. 2, pp. 67–72, Jun. 1998.

[21] A. Gorrara, S. Grant, T. Kvalcik, S. Bakke, and P. Clark, "Designing and testing a new rotary steerable system (RSS) for the onshore drilling market," in *Proc. IADC/SPE Drilling Conf. Exhib.*, London, U.K., Mar. 2015, pp. 1–21.

[22] J. P. T. Staff, "Hybrid rotary steerable system delivers higher build rates and smoother holes," *J. Petroleum Technol.*, vol. 65, no. 4, pp. 32–34, Apr. 2013.

[23] I. Tipu *et al.*, "Bending rules with high build rate RSS," in *Proc. Abu Dhabi Int. Petroleum Exhib. Conf.*, Abu Dhabi, UAE, Nov. 2015, pp. 1–12.

[24] G. Downton and N. Hale, "Rotary steerable drilling system," U.S. Patent 8 763 725, Jul. 1, 2014.

[25] W. Davila, A. Azizov, S. Janwadkar, A. Jones, J. Fabian, and T. Rowan, "Overcoming drilling challenges in the marcellus unconventional shale play using a new steerable motor with optimized design," in *Proc. SPE/EAGE Eur. Unconventional Resour. Conf. Exhib.*, Vienna, Austria, Mar. 2012, paper SPE 151132.

[26] G. L. Cavanough, M. Kochanek, J. B. Cunningham, and I. D. Gipps, "A self-optimizing control system for hard rock percussive drilling," *IEEE/ASME Trans. Mechatronics*, vol. 13, no. 2, pp. 153–157, Apr. 2008.

**JONGHEON KIM** received the B.S. and M.S. degrees in mechanical engineering from Korea University, Seoul, South Korea, in 2010 and 2012, respectively. He is currently pursuing the Ph.D. degree with the Department of Civil and Environmental Engineering, Korea Advanced Institute of Science and Technology, Daejeon, South Korea. His current research interests include directional drilling and field robotics.

**HYUN MYUNG** received the B.S., M.S., and Ph.D. degrees in electrical engineering from the Korea Advanced Institute of Science and Technology (KAIST), Daejeon, South Korea, in 1992, 1994, and 1998, respectively. He was a Senior Researcher with the Electronics and Telecommunications Research Institute, Daejeon, from 1998 to 2002, a CTO and the Director with the Digital Contents Research Laboratory, Emersys Corporation, Daejeon, from 2002 to 2003, and a Principle Researcher with the Samsung Advanced Institute of Technology, Yongin, South Korea, from 2003 to 2008. Since 2008, he has been an Associate Professor with the Department of Civil and Environmental Engineering, KAIST, where he is currently an Adjunct Professor in the Robotics Program. His current research interests include structural health monitoring using robotics, soft computing, simultaneous localization and mapping, robot navigation, machine learning, deep learning, and swarm robot.